https://doi.org/10.5194/wes-2026-60
Preprint. Discussion started: 21 April 2026

eawe european academy of wind energy
Open Access WIND ENERGY SCIENCE DISCUSSIONS

Brief communication: A novel wake mixing phenomenon and key parameters for wake recovery of floating wind turbines subjected to surge motions

Christian W. Schulz[1,*], Michael Hölling[2], Joachim Peinke[2], and Thomas Messmer[2,*]

[1]Hamburg University of Technology, Institute for Fluid Dynamics and Ship Theory, Hamburg, Germany
[2]Carl von Ossietzky Universität Oldenburg, School of Mathematics and Science, Institute of Physics, Oldenburg, Germany
[*]Equivalent contribution

Correspondence: Christian W. Schulz (christian.schulz@tuhh.de) and Thomas Messmer (thomas.messmer@uni-oldenburg.de)

Abstract.

This letter clarifies the key parameters governing the wake recovery of a floating wind turbine undergoing surge motions. A dedicated wind-tunnel campaign covering reduced frequencies (St_p) well beyond current literature is presented. This enabled a full characterisation of the wake recovery and the discovery of a previously unreported wake mixing phenomenon. We highlight three main findings: (i) enhanced wake recovery of the surging turbine is highly sensitive to thrust; (ii) wake recovery is characterised by the ratio of motion velocity amplitude to wind speed and St_p; and (iii) a previously unreported flow phenomenon improves wake recovery when the motion frequency is slightly lower than the blade passing frequency.

1 Introduction

Since the growing interest in floating offshore wind turbines (FOWT) in the mid-2000s, two key questions have, among others, challenged the floating wind community: to what extent do inherent rotor motions of a floating turbine (induced by wind and ocean waves) impact rotor aerodynamics? And how do they impact wake dynamics? Pioneer work by Jonkman and Matha (2011) and Goupee et al. (2012) analysed the platform dynamics of different standard concepts of floating substructures. Depending on the offshore site, mooring type, substructures type and size and operating conditions (wind speed, turbulence, ocean waves, turbine operating parameters, etc.), the motions of a floating turbine might be of very different kinds, covering a large range of motion frequencies, f_p and amplitudes, A_p, in the 6-degrees of freedom (DoF). Thus, rotor aerodynamics and wake dynamics might differ significantly depending on these parameters, which leads to a critical need to characterise the unsteady aerodynamic phenomena acting on rotor and wake in a broad range of motion parameters.

Sebastian and Lackner (2013) were among the first to investigate the unsteady aerodynamic effects acting on FOWT due to platform motion and found that the impact of unsteadiness on the blade loads is not only dependent on the platform motion but also varies over the blade span. A first attempt to characterise this impact by a (blade) reduced frequency was made. A possible impact on wake dynamics is also mentioned but not investigated further in the study. Later numerical and experimen-

https://doi.org/10.5194/wes-2026-60
Preprint. Discussion started: 21 April 2026

eawe european academy of wind energy
Open Access WIND ENERGY SCIENCE DISCUSSIONS

tal studies by Bayati et al. (2018); Fontanella et al. (2021); Dong and Viré (2022); Schulz et al. (2024) refined the parameters at play in motion-induced unsteady aerodynamics. From these studies, the main results were that the unsteady impact on the loads can be determined by the motion frequency, f_p, expressed in terms of the rotor reduced frequency (or platform Strouhal number), $St_p = f_p D/U_\infty$ (with D the rotor diameter and U_∞ the incoming wind speed), and - in case of tower top surge motions - the relative rotor velocity: $\Delta V^* = 2\pi f_p A_p/U_\infty$, which is the ratio of the surge velocity amplitude and the incoming wind speed. A recent numerical study by Schulz et al. (2025) applied these findings to large-scale FOWT and generalised them in terms of a characteristic thrust force response curve covering an extremely wide range of motion frequencies.

The impact of motion on the wake of a floating turbine was investigated numerically and experimentally by Rockel et al. (2014); Bayati et al. (2017); Schliffke et al. (2020); Li et al. (2022); Chen et al. (2022); Ramos-García et al. (2022); Li et al. (2024); Messmer et al. (2024). These studies converge to the following main outcomes: as for wake recovery, St_p is a key parameter. For surge and sway DoFs and $St_p \in [0.2, 0.6]$, platform motion leads to an increase in wake recovery, linked to the disturbances of near-wake structures and the formation of coherent structures induced by the rotor movements, accelerating the transport of momentum. Since platform pitch and roll motions translate to a superposition of surge/sway motions and rotations at tower-top, a comparable improvement of the wake recovery can also be expected in the case of pitch and roll motions. Moreover, as inflow turbulence intensity increases, the recovery enhancement due to platform motion decreases, eventually being negligible while the free-stream turbulence drives wake recovery Li et al. (2022); Messmer et al. (2025).

From the current literature, we identified three gaps in the knowledge of motion-induced wake recovery, which we consider as potentially relevant for the future development of floating wind. First, most studies focused on motion frequency ranges where $St_p < 1.5$, covering platform motions typical for a spar or semi-submersible FOWT at their natural frequency in surge/sway and pitch/roll around rated wind speed[1]. Especially experimental studies covering $St_p > 1.5$ are not present in current literature. However, it has recently been clarified e.g. by Schulz et al. (2025) that, for wave-induced platform motions in conjunction with today's 15 MW+ rotors, $St_p = 10$ is still within a realistic range of tower top surge and sway motions, which makes region $St_p > 1.5$ of great importance. In addition, platform motions at natural periods of TLP substructures may also enter this range. At first glance, it is tempting to think that, for such high motion frequencies, the motion's effect becomes less relevant, since the rotor is moving too fast for the wake aerodynamics to interact with the motion-induced disturbances, but we shall later see that this is not the case. Second, despite the various works investigating the wake recovery at different motion and operation parameters, it remains unclear what are the key parameters to properly characterise the motion's effect on wake recovery. In consequence, a generalised characterisation of the motion-induced wake recovery e.g., in terms of a surge-recovery curve over St_p, has not yet been derived. Third, in most studies, only one thrust coefficient $C_T = T/0.5\rho\pi(D^2/4)U_\infty^2$ was considered to investigate wake behaviour, but from anaylses of fixed wind turbine wakes (Porté-Agel et al., 2020), it is well known that the amount of momentum extracted from the wind has a significant impact on wake development.

Based on these three knowledge gaps, we designed an experimental campaign in the large wind tunnel of the University of Oldenburg utilising the TUHH model turbine (Schulz et al. (2024)) to investigate a new region of tower top surge motions up to

[1] As an example, the UMaine VolturnUS-15MW floater, which features natural frequencies of 7×10^{-3} Hz in surge/sway and 3.6×10^{-2} Hz in roll/pitch with $U_\infty \approx 10$ m/s shows $St_p \in [0.1, 0.9]$

https://doi.org/10.5194/wes-2026-60
Preprint. Discussion started: 21 April 2026

eawe european academy of wind energy
Open Access WIND ENERGY SCIENCE DISCUSSIONS

$St_p = 7$, clarify the key parameters to fully characterise the surge motion-induced wake recovery and determine its sensitivity to C_T and tip speed ratio. This letter is organised as follows: §2 details about the experimental setup, §3 presents the new results of wake profiles and recovery curves depending on St_p, ΔV^*, TSR and C_T, §4 discusses the findings and §5 contextualises them in a broader perspective.

2 Experiments

2.1 Set-up

The experiments were carried out in the large wind tunnel of the University of Oldenburg in a closed test section (width:3 m, height: 3 m, length: 30 m) without a grid generating turbulent inflow conditions. We used the TUHH rotor, a 2–bladed rotor which has a diameter $D = 2R = 0.93$ m and is mounted on a tower/hub that fits a linear actuator enabling surge motion of the rotor with frequencies f_p up to 23 Hz and amplitudes A_p up to 20 mm, see Schulz et al. (2024) for more details. The results of this letter are based on cases with an inflow wind speed U_∞ of 3 m/s and in laminar condition (i.e. with $TI_\infty = 0.3\%$). This choice of wind speed was made to broaden the St_p range, reaching St_p up to 7 at $f_p = 22.6$ Hz. Laminar conditions were chosen to isolate the motion's effect. Nevertheless, the results can be generalised to turbulent uniform inflows, however, not shown here.

Wake measurements were performed with a set of 19 hot wires aligned horizontally at hub height (1 m above the floor) and covering a width of $y \in [-2.5, 2.5]R$, similar to the measurements in Messmer et al. (2024). The hot-wires were mounted on a movable cart, enabling measurements at $x \in [1, 10]D$ (with x originating at the rotor center and aligned with the wind in downstream direction).

2.2 Cases investigated

The test campaign aimed to characterise wake recovery by independently varying key parameters influencing the near-wake flow. The wake evolution is governed by the interaction between the vortex-dominated near-wake (1–2D downstream) and the surrounding free stream while advected. The near-wake flow—determined by rotor operation and platform motion—acts as the input to this nonlinear dynamic system, while far-wake recovery represents the output. We systematically varied the near-wake flow pattern and its intensity. For surge motion at a constant rotational speed, inflow-velocity fluctuations alter blade loading and vortex strength, generating a pulsating wake. The pulsation frequency (scaled by the platform Strouhal number, St_p) controls the spatial structure, while the amplitude (scaled by ΔV^*) controls the intensity—both varied independently. Rotor operating conditions (TSR and blade pitch angle) also influence the near-wake, primarily through induction and vortex geometry. To limit complexity, TSR was varied while blade pitch was held constant, enabling different C_T to be tested.

In this study, we investigated harmonic surge motions with varying frequency of motion, f_p, and adapting A_p to maintain ΔV^* constant. f_p and A_p were varied between $[0, 22.6]$ Hz and $[0, 20]$ mm, respectively. This resulted in a range of Strouhal numbers $St_p \in [0, 7]$ and $\Delta V^* \in \{2\%, 4\%, 6\%, 8\%\}$. Most of the cases were run with a constant rotor speed $\omega = 555$ rpm,

https://doi.org/10.5194/wes-2026-60
Preprint. Discussion started: 21 April 2026

eawe european academy of wind energy
Open Access WIND ENERGY SCIENCE DISCUSSIONS

giving a tip-speed ratio of $\lambda = R\omega/U_\infty = 9$ (ω in rad/s here) and $C_T = 0.8$. For this rotational speed, the blade passing frequency is $f_b = 2\omega/60 = 18.5$ Hz. In addition, the TSR was varied between 5 and 10, which resulted in a range of $C_T \in [0.7, 0.82]$.

2.3 Recovery definition

Wake recovery, as defined in Messmer et al. (2024), gives an order of magnitude of the averaged wind speed at a given downstream location, seen by a virtual turbine aligned with the turbine generating the wake. It is defined as follows:

$$\text{Recovery}(x) = 1/D \int_{y_c-R}^{y_c+R} \overline{u}(x,y)/U_\infty dy \tag{1}$$

3 Results

3.1 Development of wake profiles and recovery

We first examine the evolution of horizontal wake wind speed profiles for $x \in [1, 10]D$ in Figure 1 (a.1) to (a.4), focusing on cases with $\Delta V^* = 4\%$ and 8% at selected Strouhal numbers up to 5.75. At $x = 1D$, the near-wake profiles (see Figure 1 (a.1)) are nearly identical for all cases, exhibiting a characteristic top-hat shape (Porté-Agel et al., 2020). The wake of the nacelle is visible in the wind profile at $x = 1D$, at the wake centre. Downstream, the profile for $St_p = 5.39$ (green, dash-dotted line) transitions to a Gaussian-like shape by $x = 4D$, while other cases retain top-hat profiles. By $x = 8D$, all wakes adopt Gaussian profiles typical of the far-wake, with most dynamic cases ($St_p > 0$) showing a profile with a smaller velocity deficit than the fixed case ($St_p = 0$). Comparing the profiles for St = 5.01, 5.39 and 5.75, one surprisingly finds a strong sensitivity on the motion frequency: $St_p = 5.39$ demonstrates the strongest recovery, while $St_p = 5.75$ (yellow dotted line) reverts to fixed-case performance.

The wake recovery (after eq. (1)) evolution against x/D in Figure 1 (b) further describes the dependency on the motion frequency in terms of St_p. In the near-wake ($x = 1D$), all cases show identical mean wind speeds, which dip slightly at $x = 2D$ before rising, marking the onset of wake recovery. Recovery is most pronounced for $St_p \in [0.3, 0.6]$, as shown in Figure 1 (b.1). For $St \in [1.0, 3.0]$ (see fig. 1b.2), the positive impact of the surge motion diminishes, while the fixed case is nearly matched at $St_p = 3.01$. However, for $St_p \in [5, 6]$, recovery suddenly increases again, peaking at $St_p = 5.39$ before collapsing when the motion frequency reaches the blade passing frequency at $St_p = St_b = \lambda \frac{n_{blades}}{\pi} = 5.75$, where the impact of the returning wake effect is strongest, see Schulz et al. (2024). St_b is the reduced frequency of the blade passing frequency, which depends on the tip speed ratio, λ and the number of blades, n_{blades}.

For $St = 0.6$ and $\Delta V^* = 4\%$ and 8% in Figure 1 (b), the case with doubled motion velocity amplitude shows a larger increase in the wake recovery, consistent with the findings of Li et al. (2022); Ramos-García et al. (2022); Messmer et al. (2024), where higher motion amplitudes tended to increase wake recovery.

https://doi.org/10.5194/wes-2026-60
Preprint. Discussion started: 21 April 2026

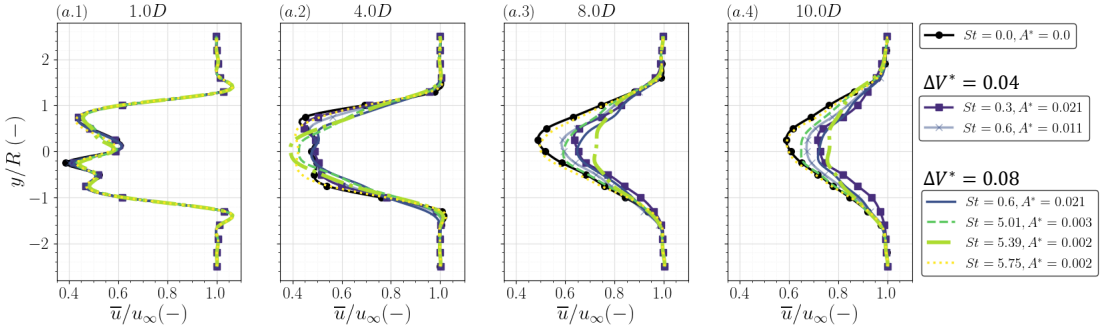

(a) Normalised wind speed wake profiles at $x \in \{1, 4, 8, 10\}D$, (a.1 to a.4) for different St and ΔV^*

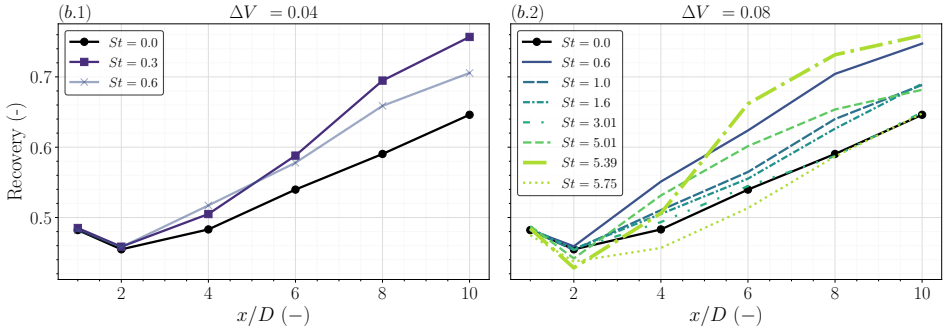

(b) Wake recovery against downstream position for cases with $\Delta V^* = 0.04$ (b.1) and $\Delta V^* = 0.08$ and different St.

Figure 1. Normalised wake profiles (a) and wake recovery against downstream position (b) for various St and ΔV^* at $TSR = 9$, $St_b = f_b D/U_\infty \approx 5.75$ and $C_T = 0.80$.

3.2 Systematic variation of surge motion parameters

The evolution of wake recovery exhibits a strong dependence on St_p and ΔV^*, particularly in the far-wake region ($x \geq 8D$). To isolate this dependence, St_p and ΔV^* were systematically varied in subsequent tests, with measurements focused at $x = 10D$. In Figure 2 (a), the resulting wake recovery is plotted as a function of the reduced frequency St_p for several values of $\Delta V^* \in [2\%, 8\%]$. Figures 2 (b, c1, d1) present selected power spectra of the streamwise velocity fluctuations in the shear layer at $y = R$ and $x \in [1, 10]D$ as done in Messmer et al. (2024). In Figures 2 (c.2–d.2), the phase-averaged velocity variation along the hot-wire array (y-axis) and the motion phase (x-axis) at $x = 4D$ is shown, following the approach of Messmer et al. (2025). Phase averaging was performed at the frequency of the highest spectral peak obtained from the power spectral densities.

For $\Delta V^* = 2\%$, an increase of wake recovery from the fixed case up to a Strouhal number of 0.3 can be observed. It is followed by a decay starting from $St_p = 0.5$. Similarly, an enhanced wake recovery and its decay towards $St_p > 1$ can be observed for the cases with higher ΔV^*. Due to limitations of the maximum surge amplitude of the actuator, the rise of the wake recovery at lower motion frequencies ($St_p \in [0.2, 0.4]$) could not be resolved experimentally for $\Delta V^* > 2\%$. The dependency of the wake recovery on St_p between 0 and 1 is in line with previous numerical and experimental findings from

https://doi.org/10.5194/wes-2026-60
Preprint. Discussion started: 21 April 2026

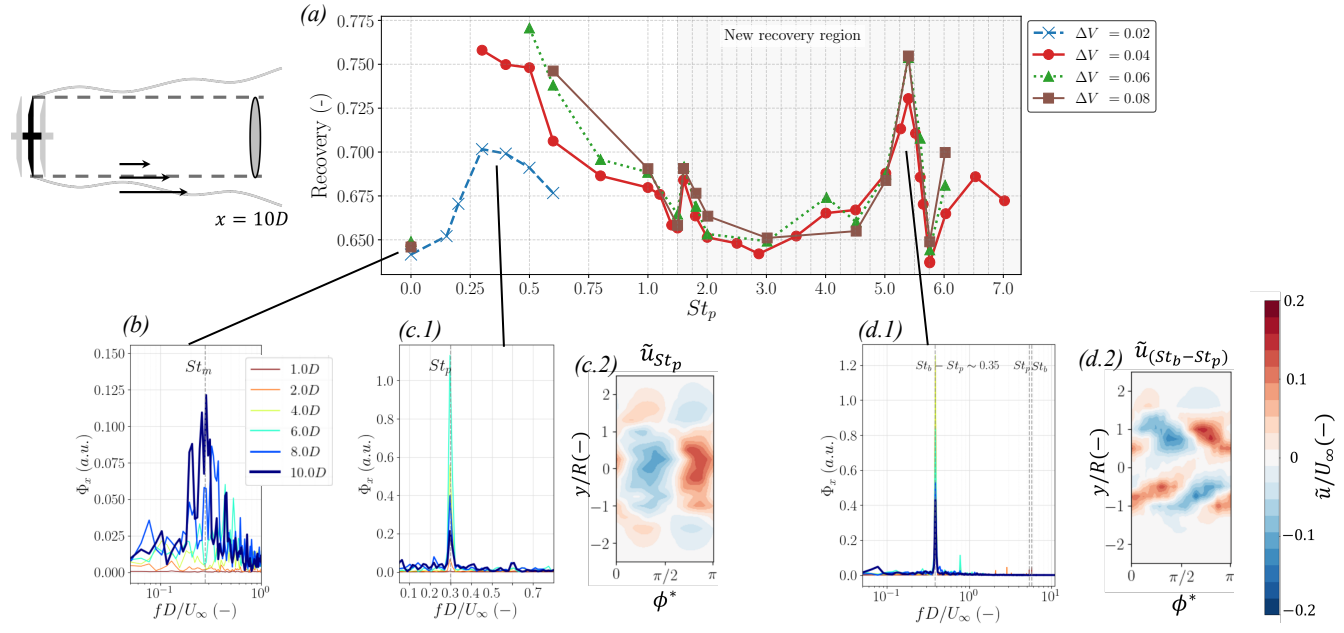

Figure 2. (a) Extended recovery curve, i.e recovery against St at $x = 10D$ for $\Delta V^* \in [0.02, 0.08]$ at $TSR = 9$, $f_b D/U_\infty \approx 5.75$ and $C_T = 0.81$. Power spectra of the wind speed fluctuation in the shear layer of the wake at $y = R$ and $x \in [1, 10]D$ for $St_p = 0$ (b), $St_p = 0.3$ (c.1) and $St_p = 5.39$ (d.1). Phase averaged of the coherent wind speed fluctuations at $x = 4D$ at $St_p = 0.3$ (c.2) and $St_b - St_p \sim 0.35$ (d.2).

Chen et al. (2022) and Messmer et al. (2024). Besides the systematic impact of St_p, a significant dependence of the strength of the wake recovery on ΔV^* can be deduced from the measurements in this St_p-regime: The higher ΔV^*, the stronger the enhancement of the wake recovery.

The power spectra of the streamwise velocity fluctuations at $St_p = 0.3$ show a dominant response at the platform motion frequency (Figure 2(c.1)), whereas the wake in the fixed case ($St_p = 0$) exhibits broadband energy distribution over $fD/U_\infty \in [0.2, 0.6]$, characteristic of natural wake meandering (Figure 2b). The forced response at $St_p = 0.3$ indicates the formation of a coherent structure responsible for enhanced wake recovery (Messmer et al., 2024), depicted in Figure 2 (c.2) at $x = 4D$.

At higher frequencies, a second increase in recovery occurs around $St_p \approx 1.5$, associated with a spectral peak at the forcing frequency and a self-generated mode at a frequency equaling $f^* D/U_\infty \approx 0.3$ (not shown here), which is similar to the quasi-periodic dynamics described by Messmer et al. (2024). For $St_p \in [2, 4]$, the recovery is nearly identical to the fixed case and shows little dependence on ΔV^*.

Surprisingly, for $St_p > 4$, the recovery increases again, especially for $St_p = 5.39$, reaching levels comparable to the optimal low-St_p regime before abruptly decreasing. The power spectra for $St_p = 5.39$ (Figure 2(d.1)) exhibits a sharp peak at a low reduced frequency $fD/U_\infty \approx 0.35$. This peak corresponds exactly to the difference between the Strouhal number related to the platform motion frequency (St_p) and the one related to the blade passing frequency (St_b). This indicates the formation of a coherent wake structure at the frequency $St_b - St_p$. The corresponding phase-averaged velocity variations (Figure 2 (d.2))

https://doi.org/10.5194/wes-2026-60
Preprint. Discussion started: 21 April 2026

eawe european academy of wind energy
Open Access WIND ENERGY SCIENCE DISCUSSIONS

show the pattern of the coherent structure with a periodicity of $St_b - St_p \approx 0.35$, although the surge motion takes place at St_p = 5.39. This pattern significantly differs from the typical pulsating mode observed at $St_p = 0.3$.

3.3 Impact of C_T and TSR

The TSR was varied ($\lambda \in [5, 10]$) to investigate the impact of different $C_T \in [0.6, 0.83]$ at a constant $\Delta V^* = 4\%$ on wake recovery at $x = 10D$. Figure 3 (a-e) shows that the wake recovery of the fixed cases ($St_p = 0$) decreases when C_T increases, since more momentum is extracted from the inflow wind. The impact of the motion on the wake recovery, which can be observed by comparing the recovery with motion to the fixed case (grey dashed line), generally diminishes with decreasing C_T (and decreasing TSR). While the trend of enhanced recovery at $St_p \approx 0.3$ is consistently observed for most cases ($C_T >= 0.76$), it nearly completely diminishes for the lowest C_T (Figure 3a). Consistent with the previous observation in Figure 2, the enhanced recovery in the high-frequency region appears at $St_b - St_p \approx 0.35$. Consequently, the minima ($St_p = St_b$) and maxima ($St_p \approx St_b - 0.35 = \lambda \frac{n_{blades}}{\pi} - 0.35$) associated with this effect move to lower motion frequencies with decreasing TSR.

4 Discussion

Consistent with previous studies focused on $St_p \in [0, 0.6]$ (Chen et al., 2022; Li et al., 2024; Messmer et al., 2024), the results show that motions with $St_p \approx 0.3$ yield the strongest recovery enhancement, while an increased motion amplitude tends to amplify this. Similar experiments by Fontanella et al. (2025) recently revealed an increased level of turbulence in the wake at 3 and $5D$ caused by surge motions. Although only limited impact of the motion on the wake recovery was found at these distances, Fontanella et al. (2025) conclude that the increased turbulence might lead to an enhanced wake recovery further downstream, which is in line with our observations.

In this study, the systematic variation of the motion parameters St_p and ΔV^* over a wide range, not previously studied in the literature, clarifies the resulting impact on wake recovery. The results in Figure 2 (a) show a clear indication, that these two parameters indeed characterise the surge-induced wake recovery: While the appearance of minima and maxima and the shape of the recovery curve are determined by St_p in all cases, the intensity of the recovery enhancement at the maxima is driven by ΔV^*.

The measurements revealed a significantly enhanced wake recovery starting at high-frequent, but still realistic, surge motions with St_p peaking when $\Delta S = St_b - St_p \approx 0.35$. This new phenomenon has, to the best of the authors' knowledge, not been described in previous literature. The fact that this peak occurs near $\Delta S \sim 0.3$ suggests that the coupling between platform motion and rotor rotation excites a natural mode of the wake, since a Strouhal number of 0.3 is associated with large energy in the wake of the fixed turbine (see Figure 2b). However, since $\Delta S \approx 0.35$ is the measurement point closest to 0.3, the maximum wake recovery occurs at this point. It is fascinating to find that the interaction between surge motion and rotor rotation has such a significant effect on the wake at a location so far from the turbine rotor, namely at $x = 10D$ (Figure 2(d.1)).

https://doi.org/10.5194/wes-2026-60
Preprint. Discussion started: 21 April 2026

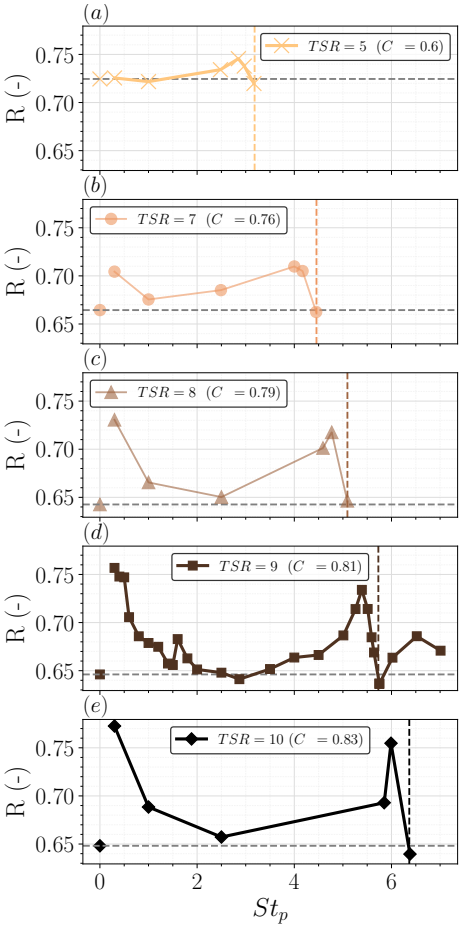

Figure 3. Recovery (R) against reduced frequency St_p, for $TSR \in [5, 10]$ giving different blade passing frequency f_b (represented by the vertical dashed line) and different rotor loadings, $C_T \in [0.6, 0.83]$.

Our current hypothesis to explain this flow phenomenon is as follows: Since it was shown that the returning wake effect significantly impacts the loading of large-scale and model-scale rotors (Schulz et al. (2024, 2025)) when the motion frequency equals the blade passing frequency, this new phenomenon is likely related to the returning wake effect. When the returning wake effect occurs at $St_p = St_b$, vortices shed from the trailing edge of the blades form a distinct pattern in the wake so that positive and negative vortices occur at the same azimuth angles in every motion period, respectively. Assuming that a minimum of wake velocity occurs at 0°, another minimum would appear at the opposite side of the rotor (180°), while the maxima occur at 90° and 270° (for a 2-bladed rotor). Since the vortices are emitted at the exact same azimuth angle in every surge motion cycle, this flow pattern is persistent across the whole wake. Introducing a slight difference between the blade passing frequency and the platform motion frequency, the generated flow pattern rotates around the rotor axis by a few degrees in every surge motion cycle. As a result, minima and maxima are distributed along a helix with increasing distance from the rotor. The

https://doi.org/10.5194/wes-2026-60
Preprint. Discussion started: 21 April 2026

eawe european academy of wind energy
Open Access WIND ENERGY SCIENCE DISCUSSIONS

frequency at which this helix rotates equals $St_{helix} = St_p - St_b$. When $St_{helix} \sim 0.3$, the helix excites a natural mode of the wake, leading to the enhanced recovery. Following this hypothesis, another peak should appear at $St_p - St_b \sim -0.3$. This could not be confirmed as this case was not considered in the experiments. If this hypothesis holds, the near-field flow pattern at the peak recovery resulting from the surge motion under the action of the returning wake effect would be a similar kind of flow pattern as created by the helix wake mixing strategy (Frederik et al., 2020). Consequently, the helix wake mixing strategy and the peak recovery from surge motions at $St_p - St_b \sim 0.3$ would be based on the same interaction phenomenon of wake and free stream, while the similar near-field flow patterns are created in two different ways. However, whether this assumption is correct remains to be verified.

It is remarkable to observe that, for all considered cases, the mean flow velocity near the rotor (1D, see Figure 1 (a.1)) is nearly identical, while significant differences arise in the development of the wake structure with increasing distance to the rotor. This gives a hint on the non-linear dynamic nature of the underlying physical phenomena: A small excitation in form of a low-frequent wake pattern such as a pulsating or helical structure becomes extremely amplified in case it appears in a suitable frequency region (around $St_p = 0.3$ in this case). Such suitable wake pattern can obviously also be be created by a combination of Again, this supports the suitability of the approach to consider the wind turbine wake as a non-linear dynamic system with the near-field flow pattern as most important input.

Another key result of these experiments is the strong sensitivity of wake recovery to the thrust coefficient. For cases with identical St_p and ΔV^*, Figure 3 shows that even small variations in C_T lead to markedly different wake recovery responses. When C_T is low (here $C_T = 0.6$), recovery enhancement is strongly reduced, whereas moderately higher values ($C_T \gtrsim 0.79$) result in significantly increased recovery of the surging turbine compared to the fixed case. This highlights the fundamental role of the mean axial induction in wake dynamics and recovery. At low C_T, the induced velocity deficit is weaker, reducing the shear between the wake and the ambient flow. Early studies on porous disks (Cannon et al., 1993) showed that such weakly sheared wakes exhibit limited dynamics, as the flow is relatively stable. As C_T increases, both induction and shear increase, leading to sharper velocity gradients and more unstable shear layers that are more susceptible to reacting to small excitation and forming large-scale coherent structures However, since this study did not vary C_T and TSR independently, it cannot be ruled out that the TSR itself might also have an impact on the observed behaviour.

5 Conclusions

This Letter investigates the impact of surge motion on wake recovery of a model wind turbine using wind tunnel experiments. The unique experimental setup allowed to increase the range of motion frequencies up to a platform Strouhal number of 7, exceeding the range of previous experiments by more than a factor of three. Three main conclusions emerge regarding the dependence of wake recovery on operation and motion parameters:

- Motion-induced wake recovery is governed jointly by the reduced frequency St_p and the normalised velocity amplitude ΔV^*. Increasing ΔV^* enhances induction fluctuations and strengthens the forcing of the wake, while the shape of the near-field flow pattern is determined by St_p. For $St_p \in [0, 0.6]$, wake recovery exhibits a largely universal behaviour,

https://doi.org/10.5194/wes-2026-60
Preprint. Discussion started: 21 April 2026

eawe european academy of wind energy
Open Access WIND ENERGY SCIENCE DISCUSSIONS

with an optimum for $St_p \in [0.3, 0.5]$, consistent with earlier work and associated with the formation of motion-induced coherent structures. At higher St_p, the response depends on additional parameters such as rotor rotation and blade number.

- Wake recovery enhancement due to surge motion is highly sensitive to the thrust coefficient C_T. Small variations in C_T lead to markedly different responses: while $C_T = 0.6$ results in negligible recovery enhancement (less than 3% compared to the fixed case), $C_T = 0.81$ yields a substantial increase (exceeding 15%). Higher C_T produces stronger shear and more unstable shear layers, which respond more effectively to surge excitation. The pronounced impact of such small changes in C_T highlights the critical role of mean induction in wake dynamics.

- A previously unreported regime of enhanced wake recovery is identified when the surge frequency approaches the blade rotation frequency St_b. In particular, maximum enhancement occurs for $\Delta S = St_b - St_p \sim 0.3$. This regime is associated with the emergence of a distinct coherent structure linked to the interaction between surge motion and rotor rotation, which may be interpreted as a helical-like wake mode. This newly identified mechanism is of direct relevance for floating wind turbines and may play an important role for large-scale FOWT.

The main trends deduced from this study persist with increasing inflow turbulence intensity up to $TI_\infty = 5\%$, although the relative impact of surge motion decreases as turbulence increases (results not shown for brevity). Future work should focus on a detailed characterisation of the newly identified mode and on assessing its robustness under more complex inflow conditions, including shear, higher turbulence levels, and large-scale flow structures.

Author contributions. CS and TM designed and carried out the experiments, analysed and interpreted the data, wrote the manuscript. MH supported the experiments, analysis and interpretation of the results and writing. JP supported the analysis and interpretation of the results and writing.

Competing interests. At least one of the (co-)authors is a member of the editorial board of *Wind Energy Science*.

Acknowledgements. The authors would like to thank K. Silwal, A. Hölling, K. Wieczorek and S. Netzband for their support before and during the experiments. The authors gratefully acknowledge the support of the Federal Ministry for Economic Affairs and Energy (BMWE) enabling the participation in the IEA Wind TCP Tasks 30 and 56. Parts of this research and the wind turbine model have been supported by the Federal Ministry for Economic Affairs and Energy (BMWE) by funding the HyStOH (grant no. 03SX409B) and the ProHyGen (grant no. 03EI3084C) projects.

https://doi.org/10.5194/wes-2026-60
Preprint. Discussion started: 21 April 2026

eawe european academy of wind energy
Open Access WIND ENERGY SCIENCE DISCUSSIONS

References

Bayati, I., Belloli, M., Bernini, L., and Zasso, A.: Wind tunnel wake measurements of floating offshore wind turbines, Energy Procedia, 137, 214–222, 2017.

Bayati, I., Belloli, M., Bernini, L., Boldrin, D. M., Boorsma, K., Caboni, M., Cormier, M., Mikkelsen, R., Lutz, T., and Zasso, A.: UNAFLOW project: UNsteady aerodynamics of FLOating wind turbines, in: Journal of Physics: Conference Series, vol. 1037, p. 072037, IOP Publishing, 2018.

Cannon, S., Champagne, F., and Glezer, A.: Observations of large-scale structures in wakes behind axisymmetric bodies, Experiments in Fluids, 14, 447–450, 1993.

Chen, G., Liang, X.-F., and Li, X.-B.: Modelling of wake dynamics and instabilities of a floating horizontal-axis wind turbine under surge motion, Energy, 239, 122 110, 2022.

Dong, J. and Viré, A.: The aerodynamics of floating offshore wind turbines in different working states during surge motion, Renewable Energy, 195, 1125–1136, 2022.

Fontanella, A., Bayati, I., Mikkelsen, R., Belloli, M., and Zasso, A.: UNAFLOW: a holistic experiment about the aerodynamics of floating wind turbines under imposed surge motion, Wind Energy Science, 6, 1169–1190, 2021.

Fontanella, A., Fusetti, A., Cioni, S., Papi, F., Muggiasca, S., Persico, G., Dossena, V., Bianchini, A., and Belloli, M.: Wake development in floating wind turbines: new insights and an open dataset from wind tunnel experiments, Wind Energy Science, 10, 1369–1387, 2025.

Frederik, J. A., Doekemeijer, B. M., Mulders, S. P., and van Wingerden, J.-W.: The helix approach: Using dynamic individual pitch control to enhance wake mixing in wind farms, Wind Energy, 23, 1739–1751, 2020.

Goupee, A. J., Koo, B., Lambrakos, K., and Kimball, R.: Model Tests for Three Floating Wind Turbine Concepts, Offshore Technology Conference, pp. OTC–23 470–MS, 2012.

Jonkman, J. M. and Matha, D.: Dynamics of offshore floating wind turbines—analysis of three concepts, Wind Energy, 14, 557–569, 2011.

Li, Y., Yu, W., and Sarlak, H.: Wake structures and performance of wind turbine rotor with harmonic surging motions under laminar and turbulent inflows, Wind Energy, 27, 1499–1525, 2024.

Li, Z., Dong, G., and Yang, X.: Onset of wake meandering for a floating offshore wind turbine under side-to-side motion, Journal of Fluid Mechanics, 934, A29, 2022.

Messmer, T., Hölling, M., and Peinke, J.: Enhanced recovery caused by nonlinear dynamics in the wake of a floating offshore wind turbine, Journal of Fluid Mechanics, 984, A66, 2024.

Messmer, T., Peinke, J., Croce, A., and Hölling, M.: The role of motion-excited coherent structures in improved wake recovery of a floating wind turbine, Journal of Fluid Mechanics, 1018, A23, 2025.

Porté-Agel, F., Bastankhah, M., and Shamsoddin, S.: Wind-turbine and wind-farm flows: a review, Boundary-Layer Meteorology, 174, 1–59, 2020.

Ramos-García, N., Kontos, S., Pegalajar-Jurado, A., González Horcas, S., and Bredmose, H.: Investigation of the floating IEA Wind 15 MW RWT using vortex methods Part I: Flow regimes and wake recovery, Wind Energy, 25, 468–504, 2022.

Rockel, S., Camp, E., Schmidt, J., Peinke, J., Cal, R. B., and Hölling, M.: Experimental study on influence of pitch motion on the wake of a floating wind turbine model, Energies, 7, 1954–1985, 2014.

Schliffke, B., Aubrun, S., and Conan, B.: Wind tunnel study of a “floating” wind turbine’s wake in an atmospheric boundary layer with imposed characteristic surge motion, in: Journal of Physics: Conference Series, vol. 1618, p. 062015, IOP Publishing, 2020.

https://doi.org/10.5194/wes-2026-60
Preprint. Discussion started: 21 April 2026

Schulz, C. W., Netzband, S., Özinan, U., Cheng, P. W., and Abdel-Maksoud, M.: Wind turbine rotors in surge motion: new insights into unsteady aerodynamics of floating offshore wind turbines (FOWTs) from experiments and simulations, Wind Energy Science, 9, 665–695, 2024.

285 Schulz, C. W., Bergua, R., Branlard, E., Netzband, S., Jonkman, J., and Roberston, A.: Unsteady aerodynamics of large-scale floating offshore wind turbines in surge motion, Renewable Energy, p. 124977, 2025.

Sebastian, T. and Lackner, M. A.: Characterization of the unsteady aerodynamics of offshore floating wind turbines, Wind Energy, 16, 339–352, 2013.